Strong spin-phonon coupling in the geometrically frustrated pyrochlore $Y_2Ru_2O_7$

J. S. Lee and T. W. Noh
School of Physics and Research Center for Oxide Electronics, Seoul National University, Seoul 151-747, Korea

J. S. Bae and In-Sang Yang
Department of Physics, Ewha Womans University, Seoul 120-750, Korea

T. Takeda
Division of Materials Science and Engineering, Graduate School of Engineering, Hokkaido University, Hokkaido 060-8628, Japan

R. Kanno
Department of Electronic Chemistry, Interdisciplinary Graduate School of Science and Engineering, Tokyo Institute of Technology, Yokohama 226-8502, Japan

(Received 12 December 2003; revised manuscript received 18 March 2004; published 28 June 2004)

We investigated temperature-dependent infrared-active transverse phonon modes of geometrically frustrated pyrochlore $Y_2Ru_2O_7$, which exhibits a spin-glass-like transition at $T_G \sim 80$ K. According to previous neutron-scattering experiments, although $Y_2Ru_2O_7$ does not accompany any static lattice symmetry change, it has an intriguing magnetic ground state with strong antiferromagnetic correlation [M. Ito *et al.*, J. Phys. Soc. Jpn. **69**, 888 (2000)]. In our far-infrared spectra, we found seven phonon modes; thermal effects could explain the temperature dependences of three phonons, but not the other four phonons. We found that these abnormal temperature-dependent behaviors could be attributed to a strong antiferromagnetic correlation, not to a structural distortion. Using quantitative analysis, we suggested that the strong spin-phonon coupling effects should play an important role in the intriguing magnetic state of this geometrically frustrated compound.

DOI: 10.1103/PhysRevB.69.214428 PACS number(s): 78.20.−e, 78.30.−j

Recently, compounds with pyrochlore and spinel structures have been extensively investigated because of their fascinating phenomena related to the geometrical frustration (GF). In these crystal structures, the magnetic ions are located at vertices of tetrahedra, so the antiferromagnetic (AF) interaction will experience a strong GF. Although the GF makes it difficult for the AF ordering to occur, many compounds show either AF ordering or signs of strong AF correlation in spin-glass ground states.[1,2] In spite of the extensive work on these compounds, the origin of the AF ordering or the strong AF correlation still remains an open question.

Usually, the AF ordered states and the spin-glass states with strong AF correlation in GF systems accompany static local structural distortions and/or related structural symmetry changes.[2–4] Based on these experimental facts, Yamashita and Ueda recently proposed the concept of a spin-driven Jahn-Teller distortion (the so-called spin-Teller distortion). Namely, degeneracy of the spin singlets of a tetrahedron is lifted by a Jahn-Teller mechanism, which leads to a cubic-to-lower-symmetry structural transition.[5] They showed that the lattice distortion corresponding to the $q=0$ Q_v mode is responsible for the magnetic ordering in ZnV_2O_4. Similarly, Echernyshyov, Moessner, and Sondhi argued that a structural distortion related to the E_u phonon mode should contribute the Néel states observed in YMn_2 and MgV_2O_4 compounds.[6] At present, many workers consider the spin-Teller mechanism to be a prerequisite for the occurrence of the AF ordering or the strong AF correlations in the GF system.

Cubic pyrochlore ruthenate $Y_2Ru_2O_7$ can be a quite unusual compound; although it has a very strong AF correlation, it does not have any noticeable structural change. Similar to the other pyrochlore materials, this compound shows a spin-glass-like transition at T_G. Interestingly, T_G reaches as high as ~ 80 K, which is much higher than those of other pyrochlore compounds.[7] From the neutron-scattering experiments, Ito *et al.* argued that the AF correlation in the spin-glass state should be so strong that the magnetic moments at the Ru sites become aligned to form an almost long-range-ordered state.[8] In addition, they reported that such magnetic ordering does not accompany any static lattice symmetry change. In these respects, it is quite important to understand the relation between the spin and the lattice degrees of freedom in $Y_2Ru_2O_7$.

In this paper, we tried to address this intriguing issue by investigating the temperature (T) dependences of the seven infrared- (IR-) active phonon modes. Using quantitative analysis, we could obtain T dependences of phonon frequencies, widths, and strengths. As T decreases below T_G, we observed that three phonons exhibit the normal T dependences, which could be explained in terms of the thermal lattice expansion effects. On the other hand, we found that the other four phonon modes show abnormal behaviors, which seem to be related to the strong AF correlation below T_G. Based on these results, we were able to demonstrate that the coupling between the spin and the phonon degrees of freedom should be strong and that it should be closely related to the strong short-range ordering nature of the magnetic moments in this pyrochlore compound.

High-density $Y_2Ru_2O_7$ polycrystals were synthesized at 3 GPa with a solid-state reaction method.[9] Near normal incident reflectivity spectra $R(\omega)$ were measured in a wide photon energy range from 5 meV to 30 eV. The T-dependent

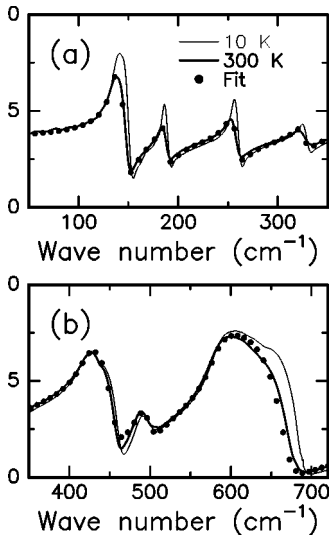

FIG. 1. $R(\omega)$ of $Y_2Ru_2O_7$ in the far-infrared region at 10 K and 300 K. Seven phonon modes contribute $R(\omega)$. The closed circles are the fitting results using the parameters listed in Table I.

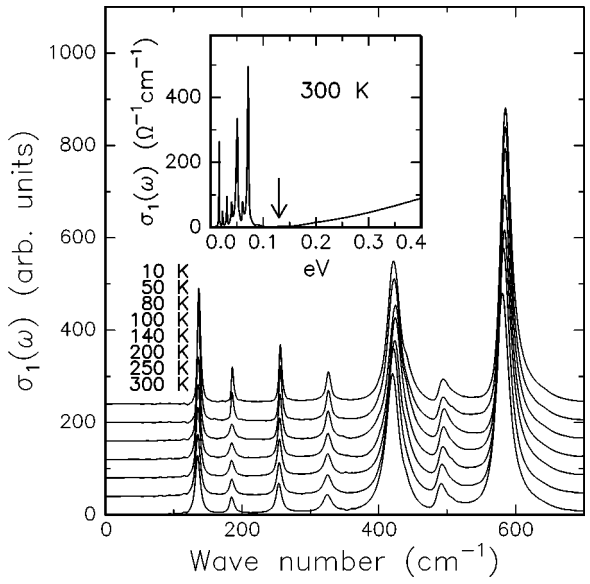

FIG. 2. Temperature-dependent $\sigma_1(\omega)$ of $Y_2Ru_2O_7$ in the far-infrared region. Seven sharp peaks ascribable to the transverse optical-phonon modes appear. The inset shows $\sigma_1(\omega)$ up to 0.4 eV where the optical gap can be estimated as around 0.14 eV, which is indicated with an arrow.

spectra were measured between 10 K and 300 K. Figure 1 shows the far-IR $R(\omega)$ at 10 K and 300 K. At both T, $R(\omega)$ show the features due to seven phonon modes. To obtain the optical conductivity spectra $\tilde{\sigma}(\omega)[=\sigma_1(\omega)+i\sigma_2(\omega)]$ from the measured $R(\omega)$, the Kramers-Kronig analysis has been commonly used using single-crystal samples. Since the pyrochlore structure is basically cubic, its optical constants should be isotropic. Thus, even for the polycrystalline samples, the Kramers-Kronig analysis could be applied. Details of the experimental process and the Kramers-Kronig analysis are described elsewhere.[10]

Figure 2 shows the T-dependent far-IR $\sigma_1(\omega)$ of $Y_2Ru_2O_7$, where seven IR-active phonon modes can be clearly seen. From a group theoretical analysis, it is well known that the 227 compounds with the $Fd\bar{3}m$ symmetry should have the zone center modes of $8F_{1u}+4F_{2u}+2F_{1g}+4F_{2g}+3E_u+E_g+A_{1g}+3A_{2u}$.[11,12] Among them, only the seven F_{1u} modes are IR-active. Consequently, the number of the observed phonons in the $Y_2Ru_2O_7$ spectra is in good agreement with the group theoretical analysis. It should be noted that no additional phonon peak appears below T_G, in agreement with the neutron-scattering data indicating no significant structural change at T_G.[8]

Figure 3 shows the T dependences of the phonon modes, which were numbered sequentially from the high to the low frequencies. For clarity, T-dependent $\sigma_1(\omega)$ are displayed with upward baseline shifts as T decreases from 300 K to 10 K. With lowering T, the anharmonic thermal motion should decrease, so the lattice constant should also decrease. Then the phonons should shift to higher frequencies and their linewidth should become narrower. The first, fourth, and fifth phonons exhibit the predicted T dependences, as shown in Figs. 3(a), 3(d), and 3(e), respectively. On the other hand, the other phonons exhibit strikingly unusual T dependences. As T decreases below T_G, the second and third phonons show discernible redshifts, as shown in Figs. 3(b) and 3(c), respectively. In addition, the sixth and the seventh phonons show abrupt decreases in their linewidths, as shown in Figs. 3(f) and 3(g), respectively. These anomalous T dependences indicate that the structural degrees of freedom should be coupled with the spin degrees of freedom in $Y_2Ru_2O_7$.

For a more quantitative analysis, we tried to fit the phonon spectra with a series of Lorentz oscillator functions of the dielectric constants,

$$\tilde{\epsilon}(\omega) = \epsilon_\infty + \sum_i \frac{S_i}{\omega_{\mathrm{Ti}}^2 - \omega^2 + i\Gamma_i\omega} = \epsilon_\infty + i\frac{4\pi}{\omega}\tilde{\sigma}(\omega), \quad (1)$$

where ϵ_∞ is the high-frequency dielectric constant, and S_i, ω_{Ti}, and Γ_i represent the strength, the frequency, and the damping constant of the ith phonon mode, respectively. Table I shows the best-fitting values of S_i, ω_{Ti}, and Γ_i at 300 K. The fitting results for $R(\omega)$ at 300 K are shown as the solid dots in Fig. 1, where ϵ_∞ was adopted as 7.8.

Although the fitting result with the Lorentz oscillators could explain the global behaviors of the phonon spectra reasonably well, there remained some differences between the experimental and the fitted data. For example, Fig. 1(b) shows that there are some deviations in the frequency regions between 450 and 500 cm^{-1} (for the second phonon) and between 600 and 700 cm^{-1} (for the first phonon). Such discrepancies could be more easily seen in $\sigma_1(\omega)$, shown in Fig. 4. (Similar discrepancies were observed for the sixth and the seventh phonons, but they are rather weak at 300 K.) Note that the first and second phonons have strongly asymmetric line shapes. We could obtain a better fitting when the Fano-type functions, such as $A(q+e)^2/(1+e^2)$, are used for $\sigma_1(\omega)$ of the asymmetric phonons.[13] The solid line in Fig. 4 shows a better agreement with the experimental data. The Fano-type dielectric functions have been used to explain in-

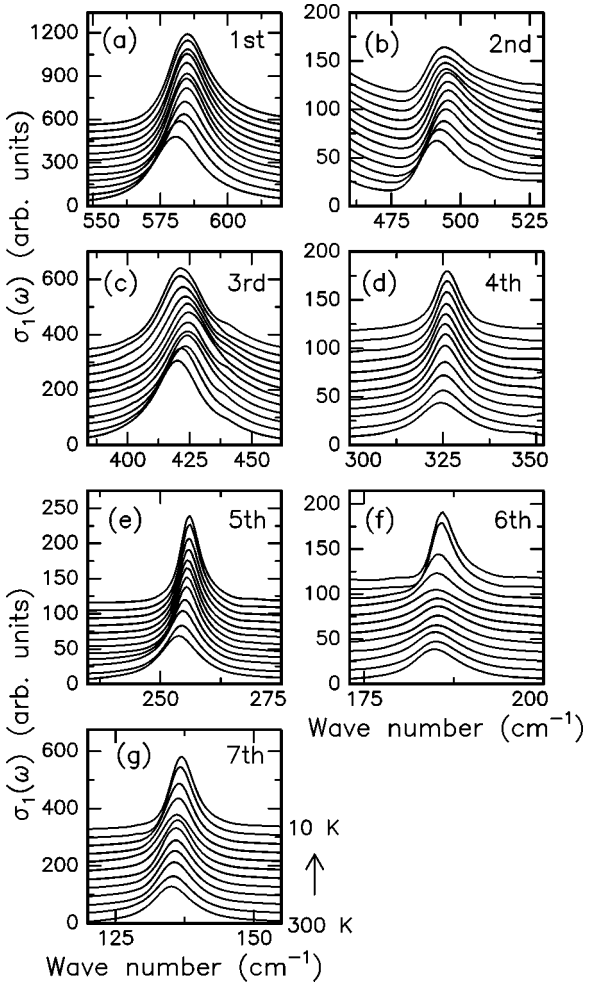

FIG. 3. *T* dependences of each phonon mode. The figures from (a) to (g) are for the phonons from the first to the seventh in order. In each figure, the spectra from top to bottom are shown for temperatures of 10, 40, 60, 70, 80, 90, 100, 120, 160, 200, 250, and 300 K.

terference effects between a sharp excitation of a phonon and a broad response.[14] Here, $e=(\omega-\omega_T)/\Gamma$, and $1/q$ is the strength of the coupling between the phonon and the broad response. The 300 K parameter values from the Fano-type fitting are also shown inside the parentheses in Table I. To

TABLE I. Values of Lorentz oscillator fitting parameters for the seven IR-active phonon modes at 300 K of $Y_2Ru_2O_7$. The values in the parentheses are fitting parameters for the Fano-type function.

	ω_{Ti} (cm^{-1})	Γ_i (cm^{-1})	S_i (Ω^{-1} cm^{-1} cm^{-1})
$i=1$ (1st)	581.0 (580.0)	21.0 (21.0)	10 150 (4.65)
$i=2$ (2nd)	492.0 (488.5)	20.0 (19.0)	1106 (6.4)
$i=3$ (3rd)	420.0	23.5	7151
$i=4$ (4th)	324.0	12.0	549
$i=5$ (5th)	253.5	11.0	729
$i=6$ (6th)	184.7 (184.8)	8.4 (8.6)	307 (0.08)
$i=7$ (7th)	135.0 (135.4)	8.0 (7.6)	1020 (0.20)

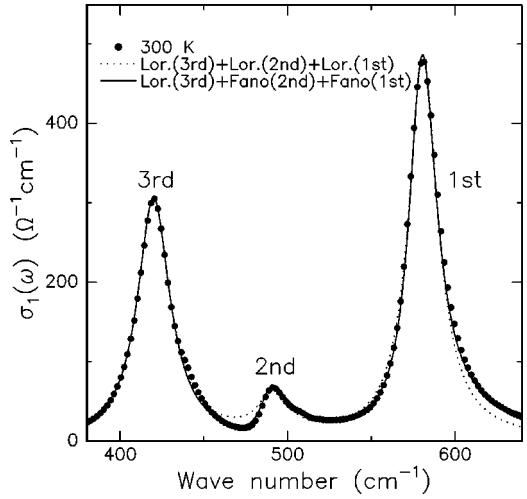

FIG. 4. Fitting results for $\sigma_1(\omega)$ at 300 K. The dotted line supposes the Lorentz oscillators for all phonon modes, and the solid line supposes the Fano-type functions for the first and second phonon modes instead of the Lorentz oscillators. All of the parameters used are listed in Table I.

see the *T* dependence of each phonon more clearly, we evaluated $\Delta\omega_{Ti}=\omega_{Ti}(T)-\omega_{Ti}(300\ \mathrm{K})$, $\Delta\Gamma_i=\Gamma_i(T)-\Gamma_i(300\ \mathrm{K})$, and $\Delta S_i=S_i(T)-S_i(300\ \mathrm{K})$.[15] The first, second, third, and fourth rows of Fig. 5 show the fitting values of $\Delta\omega_{Ti}$, $\Delta\Gamma_i/\Gamma_i(300\ \mathrm{K})$, $\Delta S_i/S_i(300\ \mathrm{K})$, and $1/q$, respectively.[16] Note that this figure was categorized into three columns, depending on the *T*-dependent behaviors, which were mentioned above.

The first column of Fig. 5 shows the *T* dependences of the phonon parameters for the first, fourth, and fifth phonons, which can be explained in terms of thermal effects reasonably well. Anharmonic interactions of the optical mode with two acoustical phonons of equal energy ($=\omega_T/2$) can provide *T*-dependent changes in ω_T and Γ,[17]

$$\omega_T = \omega_T^0 + a\left(\frac{2}{e^{\omega_T^0/2k_BT}-1}+1\right) \tag{2}$$

and

$$\Gamma = \Gamma^0 + b\left(\frac{2}{e^{\omega_T^0/2k_BT}-1}+1\right), \tag{3}$$

where ω_T^0 and Γ^0 are the harmonic frequency of the optical mode and the line broadening due to defect. *a* and *b* are the anharmonic coefficients, and $1/(e^{\omega_T^0/2k_BT}-1)$ corresponds to the thermal population factor of the acoustic modes. The solid lines in Figs. 5(a) and 5(d) correspond to the theoretical predictions based on Eqs. (2) and (3), respectively, which are in good agreement with the experimental data. Note that these phonon parameters do not show any sudden changes at T_G.

The second column shows the *T*-dependent parameters for the second and the third phonons, which have strong anomalies of ω_T at T_G. When *T* decreases from 300 K, ω_T values move to higher frequencies and their positions can be ex-

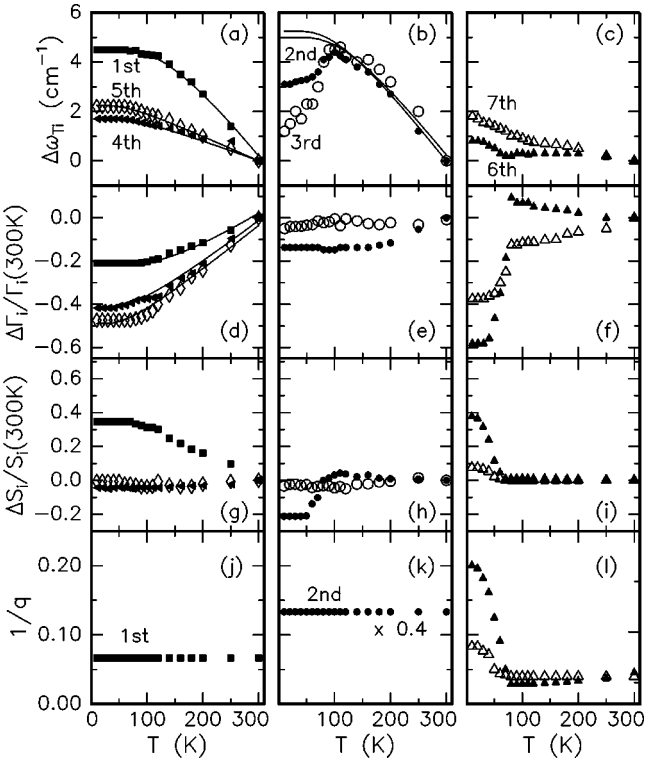

FIG. 5. The T-dependent parameters ω_T, Γ, S, and $1/q$. These are categorized into three columns, i.e., the first column for the first, fourth, and fifth phonons, the second column for the second and third phonons, and the third column for the sixth and seventh phonons, respectively. The solid lines in (a), (b), and (d) are the theoretical predictions assuming only the thermal effects. Details of each figure are described in the text.

plained in terms of Eq. (2), as shown with the solid lines in Fig. 5(b). However, below T_G, ω_T values start to deviate from the solid lines and show rather strong redshifts. Considering the fact that there is no structural change in $Y_2Ru_2O_7$ at T_G, these anomalies in ω_T should be related to the strong AF fluctuations in the spin-glass state.

The third column shows the T-dependent parameters for the sixth and the seventh phonons, which have strong anomalies of $\Delta\Gamma$ and $1/q$ at T_G. As shown in Fig. 5(f), values of $\Delta\Gamma/\Gamma(300\ \mathrm{K})$ start to show large decreases at T_G. And, as shown in Fig. 5(l), values of $1/q$ become larger, indicating that the couplings between the phonons and the broad response should become stronger. In addition, T dependences of their ω_T, shown in Fig. 5(c), cannot be simply explained in terms of Eq. (2). Note that these phonons have rather strong asymmetric Fano-type line shapes, indicating that the phonons should be coupled with a broad continuum state, which might be attributed to either electronic or magnetic origins. Note that $Y_2Ru_2O_7$ is a Mott insulator,[18] and that there are no electronic continuum states in the phonon spectral region, as shown in the inset of Fig. 2. Therefore, the continuum background might be due to a broad density of states for spin waves, and the strong anomalies related to these phonons could come from rather strong spin-phonon couplings.

The strong spin-phonon coupling could result in a shift of the phonon frequency. Let us consider that the exchange interactions between the magnetic atoms become the strongest for those located at the nearest-neighboring sites. For a displacement by x from the equilibrium position, the crystal potential U can be given by $U=\frac{1}{2}kx^2+\Sigma_{i,j}\,J_{ij}(x)\langle S_iS_j\rangle$. The second term appears, since the exchange energy constant J_{ij} is a function of the structural parameters, such as the lengths between the magnetic ions and the corresponding angles mediated by the O ions. Its second derivative, $\partial^2U/\partial x^2\approx k+\Sigma_{i,j}(\partial^2J_{ij}/\partial x^2)\langle S_iS_j\rangle$, gives the harmonic force constant. Note that the second term represents the spin-phonon coupling, which suggests that the phonon frequency should have an additional contribution $\lambda\langle S_iS_j\rangle$.[19] Here, $\langle S_iS_j\rangle$ denotes a statistical mechanical average for the adjacent spins, and λ is the spin-phonon coupling coefficient which can be different for each phonon and can have either a positive or a negative sign. Note that the T-dependent value of $\langle S_iS_j\rangle$ can be evaluated from the integrated intensities of the neutron-scattering peaks of magnetic origin.[8] By fitting with the deviation of ω_{T2} and ω_{T3} from the prediction of Eq. (2) as $\lambda\langle S_iS_j\rangle$, we found that the deviation could be explained quite well by the spin-phonon coupling term. We could also estimate that values of λ for the second and the third phonons are about 6 and 9 cm^{-1}, respectively. The magnitudes of these λ values are intermediate, compared to $|\lambda|\sim 1$ cm^{-1} for FeF_2 and MnF_2,[20] and $|\lambda|\sim 50$ cm^{-1} for CuO.[21]

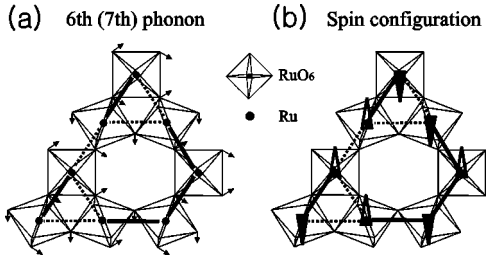

FIG. 6. (a) Atomic displacements of the sixth (seventh) phonon modes (Ref. 12). The thick bold and dotted lines connect the Ru ions with $\theta>\theta_0$ and $\theta<\theta_0$, respectively. (b) Possible spin configuration related to such atomic displacements.

How can we understand the anomalies of $\Delta\Gamma$ and $1/q$ for the sixth and the seventh phonons? Figure 6(a) shows the displacement of the oxygen ions for one of these low-frequency phonon modes.[12] Note that the exchange energy is very sensitive to the Ru-O-Ru angles θ for the superexchange interaction; while the 180° superexchange gives a negative (AF) J, the 90° superexchange provides a positive J. Note that the θ value without the lattice displacement, θ_0, is about 129°.[9] Under the lattice displacement, some of the Ru-O-Ru angles become larger than θ_0, and the others become smaller than θ_0. In Fig. 6(a), the Ru pairs with $\theta>\theta_0$ and those with $\theta<\theta_0$ are indicated by the solid and the dotted lines, respectively. With the lattice displacement, the *AF interaction* between the Ru pairs connected by the *solid* line should increase, and vice versa. Based on these changes, we could figure out a favorable spin configuration, which is displayed in Fig. 6(b). Actually, this spin configuration, obtained from a simple argument based on the superexchange changes, is similar to the spin-configuration obtained from theoretical calculations,[6] which assumed an E_u phonon-

related structural distortion while the global structural symmetry remains cubic.[6] A phonon is a quantized dynamical motion of lattice displacements; the lattice displacements, shown in Fig. 6(a), should oscillate in time. If the spin degree of freedom couples with the lattice displacements dynamically, the favorable spin configuration will change accordingly, which could correspond to a spin wave. This coupling between the lattice and the spin degrees of freedom, i.e., the so-called dynamic spin-phonon coupling,[22] could provide a possible explanation for changes in phonon dynamics due to the spin ordering. The nearly long-range AF ordering in $Y_2Ru_2O_7$ could increase the coupling between the phonon and the corresponding spin wave, resulting in the increase in $1/q$. Also, the abrupt decrease of Γ might be attributed to the reduction of the phonon decaying paths due to the occurrence of the nearly long-range magnetic ordering.[19]

As we mentioned in the Introduction, $Y_2Ru_2O_7$ is a unique compound since it shows a very strong AF correlation without any noticeable structural distortion. Our infrared studies show that such an intriguing phenomenon should be closely related to the large spin-phonon coupling effect. Although the local structural disorder and/or the chemical disorder could drive short-range magnetic ordering, such possibilities can be excluded in the $Y_2Ru_2O_7$ case for the following reasons. First, if there are local structural disorders below T_G, the phonon linewidth should be broadened accordingly. However, we found no phonon peak exhibiting the predicted linewidth broadening below T_G, indicating that the local structural disorder could not play an important role. Second, in the case of the chemical disorder, it should be noted that the pyrochlore compounds are usually free from the site disorder. In $A_2Ru_2O_7$ (A=Y and rare-earth ions), the value of T_G varies quite systematically with substitution of the A-site ion.[23] Moreover, in $Bi_xY_{2-x}Ru_2O_7$, the highest T_G appears for the $x=2.0$ compound which has the smallest disorder.[7] This suggests that the chemical disorder effect should be irrelevant to the observed strong AF correlation in $Y_2Ru_2O_7$. Therefore, the strong coupling between the spin and phonon degrees of freedom could be the most plausible origin to explain the strong AF correlation in this pyrochlore ruthenate. In order to get a more thorough understanding of the magnetic state of $Y_2Ru_2O_7$, further studies, including exact assignment of all of the phonon modes and a detailed understanding of the spin-phonon coupling mechanism, are seriously desirable.

In summary, we investigated the temperature-dependent behaviors of the transverse optical-phonon modes of $Y_2Ru_2O_7$. Through quantitative analysis, we observed strong signatures suggesting that the structural degrees of freedom are strongly coupled with the spin degrees of freedom. We proposed that the strong spin-phonon coupling effects should be closely related to the strongly AF correlation (but just a little short of forming an ordered state) observed in this geometrically frustrated system.

We would like to thank Jaejun Yu for helpful discussion. This work was supported by the Ministry of Science and Technology through the Creative Research Initiative program. The experiments at PLS were supported by MOST and POSCO.

[1] J. S. Gardner, B. D. Gaulin, S.-H. Lee, C. Broholm, N. P. Raju, and J. E. Greedan, Phys. Rev. Lett. **83**, 211 (1999).
[2] H. Mamiya, M. Onoda, T. Furubayashi, J. Tang, and I. Nakatani, J. Appl. Phys. **81**, 5289 (1997).
[3] A. Karen and J. S. Gardner, Phys. Rev. Lett. **87**, 177201 (2001); C. H. Booth, J. S. Gardner, G. H. Kwei, R. H. Heffner, F. Bridges, and M. A. Subramanian, Phys. Rev. B **62**, R755 (2000).
[4] Y. Ueda, N. Fujiwara, and H. Yasuoka, J. Phys. Soc. Jpn. **66**, 778 (1997).
[5] Y. Yamashita and K. Ueda, Phys. Rev. Lett. **85**, 4960 (2000).
[6] O. Tchernyshyov, R. Moessner, and S. L. Sondhi, Phys. Rev. Lett. **88**, 067203 (2002); Phys. Rev. B **66**, 064403 (2002).
[7] S. Yoshii and M. Sato, J. Phys. Soc. Jpn. **68**, 3034 (1999).
[8] M. Ito, Y. Yasui, M. Kanada, H. Harashina, S. Yoshii, K. Murata, M. Sato, H. Okumura, and K. Kakurai, J. Phys. Soc. Jpn. **69**, 888 (2000).
[9] R. Kanno, Y. Takeda, T. Yamamoto, Y. Kawamoto, and O. Yamamoto, J. Solid State Chem. **102**, 106 (1993).
[10] H. J. Lee, J. H. Jung, Y. S. Lee, J. S. Ahn, T. W. Noh, K. H. Kim, and S.-W. Cheong, Phys. Rev. B **60**, 5251 (1999).
[11] E. Buixaderas, S. Kamba, J. Petzelt, M. Savinov, and N. N. Kolpakova, Eur. Phys. J. B **19**, 9 (2001).
[12] N. T. Vandenborre, E. Husson, and H. Brusset, Spectrochim. Acta, Part A **37**, 113 (1981).
[13] U. Fano, Phys. Rev. **124**, 1866 (1961).
[14] A. B. Kuz'menko, D. van der Marel, P. J. M. van Bentum, E. A. Tishchenko, C. Presura, and A. A. Bush, Phys. Rev. B **63**, 094303 (2001).
[15] Compared to the Lorentz oscillator, the Fano-type function has an additional parameter q. The parameter S has a different meaning from that for the Lorentz oscillator, and it is not directly related to the strength of the peak.
[16] We have observed similar results for the Raman-active phonon modes, which will be reported elsewhere.
[17] J. Menendez and M. Cardona, Phys. Rev. B **29**, 2051 (1984), and references therein.
[18] J. S. Lee, Y. S. Lee, T. W. Noh, K. Char, Jonghyurk Park, S.-J. Oh, J.-H. Park, C. B. Eom, T. Takeda, and R. Kanno, Phys. Rev. B **64**, 245107 (2001).
[19] K. Wakamura, Solid State Commun. **71**, 1033 (1989).
[20] D. J. Lockwood, R. S. Katiyar, and V. C. Y. So, Phys. Rev. B **28**, 1983 (1983); D. J. Lockwood and M. G. Cottam, J. Appl. Phys. **64**, 5876 (1988).
[21] X. K. Chen, J. C. Irwin, and J. P. Franck, Phys. Rev. B **52**, R13 130 (1995).
[22] S. Naler, M. Rübhausen, S. Yoon, S. L. Cooper, K. H. Kim, and S. W. Cheong, Phys. Rev. B **65**, 092401 (2002).
[23] N. Taira, M. Wakeshima, and Y. Hinatsu, J. Mater. Chem. **12**, 1475 (2002).